




Simple, fast, and instrumentless fabrication of paper analytical devices by novel contact stamping method based on acrylic varnish and 3D printing

Tatiane Alfonso de Araujo¹ · Natália Canhete de Moraes² · Jacqueline Marques Petroni² · Valdir Souza Ferreira² · Bruno Gabriel Lucca² 

Received: 17 August 2021 / Accepted: 11 November 2021 / Published online: 27 November 2021
© The Author(s), under exclusive licence to Springer-Verlag GmbH Austria, part of Springer Nature 2021

Abstract

A new contact stamping method for fabrication of paper-based analytical devices (PADs) is reported. It uses an all-purpose acrylic varnish and 3D-printed stamps to pattern hydrophobic structures on paper substrates. The use of 3D printing allows quickly prototyping the desired stamp shape without resorting to third-party services, which are often expensive and time consuming. To the best of our knowledge, this is the first report regarding the use of this material for creation of hydrophobic barriers in paper substrates, as well as this 3D printing-based stamping method. The acrylic varnish was characterized and the features of the stamping method were studied. The PADs developed here presented better compatibility with organic solvents and surfactants compared with similar protocols. Furthermore, the use of this contact stamping method for fabrication of paper electrochemical devices was also possible, as well as multiplexed microfluidic devices for lateral flow testing. The analytical applicability of the varnish-based PADs was demonstrated through the image-based colorimetric quantification of iron in pharmaceutical samples. A limit of detection of 0.61 mg L⁻¹ was achieved. The results were compared with spectrophotometry for validation and presented great concordance (relative error was < 5% and recoveries were between 104 and 108%). Thus, taking into account the performance of the devices explored here, we believe this novel contact stamping method is a very interesting alternative for production of PADs, exhibiting great potentiality. In addition, this work brings a new application of 3D printing in analytical sciences.

Keywords 3D printing · Colorimetric detection · Electrochemical device · Iron determination · Microfluidics · Pharmaceutical analysis

Introduction

The development of simple, miniaturized, and low-cost devices targeting point-of-need analytical systems has gained great attention in the last years [1]. Towards to this, microfluidic paper analytical devices (μ PADs) emerged as one of the most explored analytical platforms for applications in areas such as clinical diagnosis [2], environmental sciences [3], biological analysis [4], and forensics [5].

Some key points responsible for expanding the popularity of μ PADs are the minimal consumption of reagents, cheapness, easy acquisition worldwide, and the capability to drive fluids by capillary forces without dedicated instrumentation [6]. These attributes make paper analytical devices (PADs) an interesting choice for analytical procedures in resource-constrained locations [7]. A wide variety of techniques have been used for detection in PADs, such as colorimetry and electrochemical sensing. Image-based colorimetric detection is the most used due to its intuitiveness, simplicity, speed, and low cost [8]. Electrochemical detection is also widely explored as it provides good sensitivity, possibility of miniaturization, and portability [9].

The patterning of hydrophobic barriers on paper substrates is an essential step when fabricating PADs. These barriers define the zones where the liquids can go and prevent unwanted spreads [10]. The most commonly used

✉ Bruno Gabriel Lucca
bruno.lucca@ufms.br

¹ Instituto Federal de Educação, Ciência e Tecnologia de Mato Grosso Do Sul, Campo Grande, MS 79100-510, Brazil

² Instituto de Química, Universidade Federal de Mato Grosso Do Sul, Campo Grande, MS 79074-460, Brazil

protocols for forming hydrophobic structures on paper substrates include wax printing [11], screen-printing [12], cutting methods [13], photolithographic methods [8], microembossing [14], coating methods [15], and contact stamping-based methods [16]. Here it is interesting to highlight that, despite their effectiveness, these methods often require dedicated electrical instrumentation such as plotters, ovens, cutters, and printers, in addition to procedures such as baking, curing, heating, laminating, and developing.

Focusing on stamping-based methods, there are reports in literature of procedures that use materials such as indelible ink [16], wax [17], nail polish [18], vegetal resin [19], and poly(dimethylsiloxane) (PDMS) [20] to create the hydrophobic structures. Some drawbacks of these approaches are the large number of steps required, necessity of expensive benchtop equipment, and narrow chemical resistance against organic media and surfactants. Considering these points raised, it is correct to state that the reporting of fast, simple, and instrument-free protocols for fabrication of PADs is an important contribution to this research area. Likewise, the employment of new materials with greater chemical resistance to obtain hydrophobic barriers in paper substrates is also an equally important issue.

Iron is one of the most abundant elements on earth and also the most abundant metal in the human body. Iron is essential for our health and plays an important role in various metabolic processes, such as the regulation of osmotic pressure in cells, respiration, and oxygen transport. Iron supplementation can be accomplished, among other ways, by taking oral supplements. The sensing of iron in such products is relevant as it assures the compliance and quality control. While iron deficiency causes anemia, large amounts of iron can lead to oxidative stress, DNA damage, liver damage, and hepatitis [21–23].

In this panorama, this work shows for the first time the application of an all-purpose varnish for patterning hydrophobic barriers aiming functional paper-analytical devices. This inexpensive varnish based on acrylic resin is widely used in craftwork worldwide. A fabrication protocol based on the use of reusable 3D-printed stamps was developed. Here, fused deposition modeling (FDM) 3D printing technique was employed. It consists on the production of three-dimensional structures by adding layers of thermoplastic materials such as acrylonitrile butadiene styrene (ABS) and polylactic acid (PLA) that are continuously extruded through a heated nozzle [24]. The widespread use of 3D printing in analytical chemistry has been exhaustively demonstrated in many recent works and has brought great improvements [25].

Some benefits of this novel contact stamping approach over similar protocols are the simplicity, low cost, and the fact that it is instrumentless. The method consists of only one quick stamping step and does not utilize any equipment

nor require additional procedures. As far as we know, this is one of the fastest, simplest, and cheapest methods for fabrication of PADs. The varnish composition was characterized and the method was meticulously investigated. The varnish-based hydrophobic barriers showed better chemical resistance to organic solvents and surfactants compared to other approaches. Furthermore, the stamping method presented here can also be employed in the fabrication of paper electrochemical devices.

The analytical applicability of this approach was explored through colorimetric determination of iron in pharmaceutical formulations. The results obtained in the determinations were compared with spectrophotometry and presented great concordance. Thus, based on what has been described here, we believe that this new contact stamping approach based on all-purpose varnish and 3D printing demonstrates great feasibility on fabrication of point-of-need devices, especially for resource-constrained regions.

Materials and methods

Chemicals and materials

All the chemicals employed here were analytical grade and used in the way they were received: acetone (99.5% purity), acetonitrile (99.5% purity), dimethylformamide (DMF, 99.8% purity), dimethylsulfoxide (DMSO, 99.9% purity), ethanol (99.5% purity), methanol (99.8% purity), acetic acid (99.5% purity), and hydrochloric acid (37% concentration) were purchased from Dinâmica (Diadema, SP, Brazil). Triton X-100 (TX-100, 98% purity) was provided by Acros Organics (Geel, Belgium). SERVA (Heidelberg, Germany) supplied cetyltrimethylammonium bromide (CTAB, 99% purity). Sodium dodecyl sulfate (SDS, 99% purity) was acquired from Sigma-Aldrich (Saint Louis, MO, USA). Potassium chloride (99% purity), sodium hydroxide (97% purity), potassium hexacyanoferrate(II) (98.5% purity), potassium hexacyanoferrate(III) (99% purity), iron(II) chloride (97% purity), sodium acetate (98% purity), ortho-phenanthroline (99% purity), and hydroxylamine (99% purity) were purchased from Neon (Suzano, SP, Brazil). All-purpose acrylic varnish was obtained from Acrilex (São Bernardo do Campo, SP, Brazil). Food dye, ashless quantitative filter paper, tracing paper (A4, 180 g/m²), 6B grade pencil, polyester film (A4), thermal laminating pouch film (A4), and adhesive tape were acquired at local stores. Acrylonitrile butadiene styrene (ABS) filament (1.75-mm diameter) was provided by 3DFila (Belo Horizonte, MG, Brazil). All the aqueous solutions used here were prepared with purified water (resistivity ≥ 18.2 M Ω cm) provided by a Permuton RO0310 reverse osmosis water purifier system (Curitiba, PR, Brazil).

Instrumentation

The electrochemical experiments were carried out at room temperature using an Autolab PGSTAT128N potentiostat/galvanostat (Ecochemie, Utrecht, The Netherlands) connected to a computer and managed by Metrohm Autolab Nova 2.1 software. The morphological analysis was performed by scanning electron microscopy (SEM) utilizing a JSM-6380LV instrument (Jeol, Tokyo, Japan). The Fourier transform infrared (FTIR) measurements were carried out on a Tensor 27 infrared spectrometer (Bruker, Billerica, MA, USA). Kasvi K37-VIS spectrophotometer (Kasvi, São José dos Pinhais, PR, Brazil) was employed for the spectrophotometric measurements. A Crealty Ender 3 FDM 3D printer (Crealty, Shenzhen, China) equipped with a 0.4-mm diameter brass extruder nozzle was used to produce the 3D-printed parts. The 3D prints were performed at 0.20-mm layer resolution, 15-mm s⁻¹ printing speed, and 50% infill. A Goldmaq PS-380 office laminator (Gold Maq, Goiânia, GO, Brazil) and a Silhouette Cameo 3 cutting plotter (Silhouette Brasil, Belo Horizonte, MG, Brazil) were utilized during the fabrication of the electrochemical devices. Scanned images of the PADs were obtained using a Lexmark MX622 multifunctional printer (Lexmark, Lexington, KY, USA).

Fabrication of the PADs

Figure 1 describes the procedure for manufacturing the PADs: (a) first, the 3D model of the stamps (e.g., hollow cylinders with 7-mm inner diameter × 1-mm wall thickness × 35-mm height) is designed utilizing Fusion 360 free 3D CAD/CAM software (Autodesk, San Rafael, CA, USA). After, the CAD file is converted to STL format and processed using Ultimaker Cura 3.6 software (Geldermalsen,

The Netherlands) to generate the GCODE file with the print commands. The stamps are then printed in ABS using a FDM 3D printer; (b) a small amount (thin film) of the all-purpose varnish is poured onto a Petri dish to serve as a stamp pad for the 3D-printed stamps; (c) after immersing the 3D-printed stamp into the Petri dish, the hydrophobic barriers are created on quantitative filter paper substrate by stamping and pressing for 2 s; (d) after drying at room temperature for 10 min, the solvent evaporates and the PADs are ready for use. This method allows the production of functional colorimetric and electrochemical paper-based devices. Posteriorly to the use, the 3D-printed stamps can be cleaned and reused multiple times.

Iron quantitative colorimetric assay

In order to demonstrate the analytical feasibility of the PADs developed here, spot tests fabricated by the proposed method were utilized for colorimetric quantification of iron ions in pharmaceutical samples. The determination was based on the reaction between ferrous ion and phenanthroline, which generates an orange-red complex that is highly stable in pH range between 3.0 and 4.5 [26]. The chromogenic reagent utilized consisted of a 0.03 mol L⁻¹ ortho-phenanthroline and 0.1 mol L⁻¹ hydroxylamine prepared in a 0.2 mol L⁻¹ acetate buffer aqueous solution (pH = 4.4). For the colorimetric assays, an optimized volume of 8 μL of the chromogenic reagent was spotted into the detection zones of the PADs and allowed to dry at room temperature for 10 min. Subsequently, 8 μL of Fe²⁺ standard solution or sample solutions was spotted into these detection zones and dried at room temperature for another 10 min. After this protocol, the devices were scanned and the image-based color measurements were carried out.

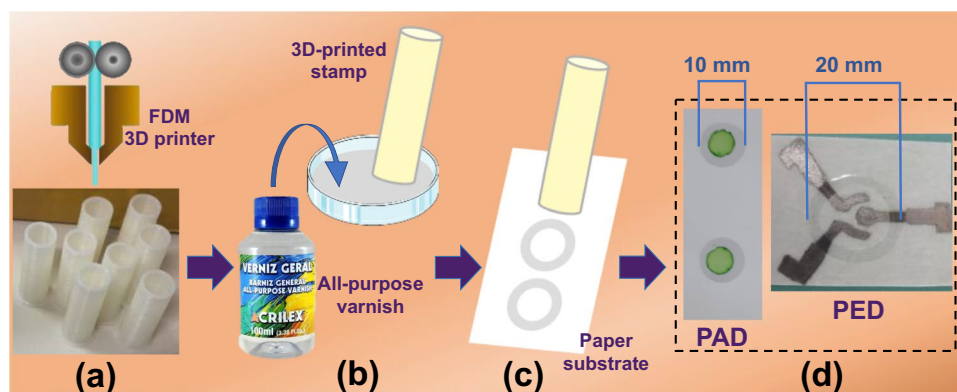


Fig. 1 Steps for production of the paper-based devices: (a) the stamps are projected according to the desired design and printed in ABS using a FDM 3D printer; (b) to facilitate the handling, the varnish is poured onto a Petri dish, which serves as a stamping pad; (c) after immersing the 3D-printed stamp into this stamp pad, hydrophobic

barriers are created on quantitative filter paper by stamping and pressing for 2 s; (d) after resting for 10 min to evaporate the solvent, functional devices suitable for colorimetric and electrochemical assays are obtained

Pharmaceutical samples

Three samples of commercial drugs used to treat anemia containing different dosages of iron(II) were prepared according to the following procedure: first, five pills of each pharmaceutical product were crushed with the aid of a mortar and pestle. During this step, the “peel” that covers the tablets was carefully removed using tweezers. The crushed pills were then diluted in 100-mL volumetric flasks and sonicated for 10 min. Afterwards, small fractions of the supernatants were filtered through 0.22- μm membrane syringe filter and diluted in 10-mL volumetric flasks. These latter solutions of the three samples were then submitted to the colorimetric measurements.

Image capture and analysis

For the quantitative colorimetric measurements of iron(II) ion, the digitalized images of the PADs were analyzed using Corel Photo-Paint software (Corel Corporation, ON, Canada). The images were first imported into the software and then converted to CMYK (32 bits). The magenta channel of the histogram tool was utilized for the measurements. The analytical signal consisted of the arithmetic mean of color intensity within each PAD detection zone [10, 27].

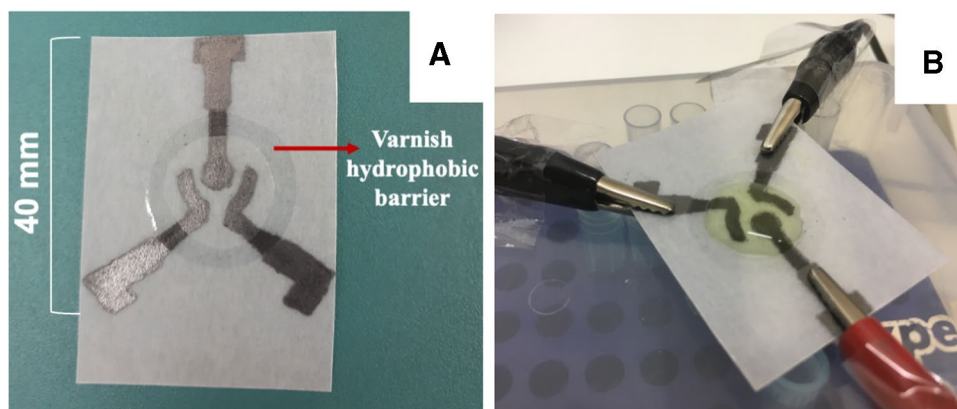
Validation experiments

The pharmaceutical samples were also analyzed by spectrophotometry to validate the results obtained with the image-based colorimetric method. For the spectrophotometric measurements, 3-mL aliquots of the chromogenic reagent (0.03 mol L^{-1} ortho-phenanthroline and 0.1 mol L^{-1} hydroxylamine prepared in 0.2 mol L^{-1} acetate buffer at $\text{pH}=4.4$) were mixed with 1-mL aliquots of Fe^{2+} standard solutions or sample solutions and diluted to 5 mL. Thereafter, *ca.* 3 mL of these solutions was transferred to cuvettes and measurements were carried out at 510-nm wavelength [28].

Electrochemical measurements

The contact stamping method proposed here was also explored in the production of paper electrochemical devices (PEDs) that were used in cyclic voltammetry (CV) measurements. The PED was fabricated in tracing paper utilizing the all-purpose acrylic varnish to create a hydrophobic barrier that has the role of preventing the leakage of the solutions and delimiting the geometric area of the electrochemical cell. The fabrication protocol was based in a previous report of our group [29]. Briefly, the bottom side of the tracing paper is first sealed against the thermal laminating pouch film using an office laminator at temperature of $80 \text{ }^\circ\text{C}$; then, the working, counter, and pseudo-reference carbon electrodes are hand-drawn on the opposite side of tracing paper utilizing the 6B grade pencil and a polyester mold containing the desired layout previously fabricated on a cutting plotter; during this step, a multimeter is employed to monitor the electrical resistance of the electrodes and ensure the reproducibility; the last step is to demarcate the geometric area of the paper-based electrochemical cell: for this, 3D-printed cylindrical stamps with 16-mm inner diameter and 1-mm wall thickness are used to stamp the all-purpose varnish hydrophobic barriers directly over the PEDs. After drying for 10 min at room temperature, the PEDs are ready to use. Each PED has the dimensions of *ca.* $40 \times 40 \text{ mm}$ and an estimated cost of *ca.* $\$ 0.04$. The diameter of the working electrode is 5 mm and the maximum volume of the paper-based cell is *ca.* $300 \mu\text{L}$. During the measurements, electrical connections are directly clamped to the PED, such as shown in Fig. 2.

Fig. 2 Picture of the PED fabricated by the contact stamping method developed (A); PED connected to the potentiostat, such as used in the experiments, demonstrating the effectiveness of the varnish hydrophobic barrier in retaining the solution into the paper electrochemical cell (B)



Results and discussion

Characterization of the material and comparison with other approaches

In this work, we first demonstrate the fabrication of μ PADs using an all-purpose varnish to create the hydrophobic barriers. This low-cost liquid varnish is commonly utilized to protect and waterproof craftworks made in paper, wood, glass, ceramics, plastic, polystyrene, and canvas. As stated in the Safety Data Sheet (SDS), this varnish is composed of a thermoplastic acrylic resin ($\approx 40\%$) solubilized in an appropriate solvent ($\approx 60\%$). It may be injurious and cause irritation to eyes and skin besides being harmful to aquatic organisms. FTIR provided more detailed information about the chemical composition of the material. Strong absorption bands at 1148 and 1728 cm^{-1} can be associated to the C-O and C=O stretching bands, respectively. Furthermore, the small band at 1608 cm^{-1} and the medium band at 2962 cm^{-1} can be attributed to the respective C=C and C-H stretching bands. It confirms the presence of acrylate groups and aromatic hydrocarbons. The full FTIR spectrum is shown in Fig. S1 (Electronic Supporting Information (ESI)).

The instrumentless procedure developed here is based on the use of inexpensive 3D-printed stamps to produce varnish hydrophobic barriers on paper substrates. As this liquid varnish has a relatively low viscosity (≈ 200 cP), its penetration into the paper fibers to form hydrophobic barriers is favored. Some clear advantages of the approach reported here are simplicity and low cost, which make it an interesting choice for resource-constrained locations. The cost per device fabricated by this method was calculated to be *ca.* \$ 0.004, which is extremely cheap. Moreover, it does not need any instrumentation or procedures often utilized in the fabrication of PADs such as baking, curing, heating, laminating, or developing. To better scrutinize the key points related to this method, Table 1 brings a comparison with other stamping methods used to produce hydrophobic barriers in PADs.

Evaluation of the hydrophobic barriers and paper devices

Initial tests and resolution limits

Initially, the feasibility of the all-purpose varnish for creating hydrophobic barriers on paper substrates was investigated. The varnish was used in its original form and stamped over quantitative filter paper. After drying at room temperature, the hydrophobicity of the barriers

was tested using food dye aqueous solution. As can be observed in Fig. S2 (ESI), the varnish barrier showed good hydrophobicity, sealing the paper, and avoiding the absorption of the solution. This finding demonstrates the potential for use of this material in the production of paper analytical devices. For the subsequent studies, the stamping and drying time were evaluated. It was found that a stamping time of 2 s yielded the best results (solid hydrophobic barriers with less dispersion of the varnish) and the varnish solvent evaporated completely after 10 min, generating ready-to-use devices.

The resolution of the proposed method for the production of spot tests and fluidic channels was evaluated. Figure 3A and 3B present spot tests with internal diameter between 2 and 7 mm, as well as flow channels with widths in the range from 2 to 5 mm. For both devices, it can be seen that the minimal stamp dimension that allowed complete flow of solutions without obstruction was 3 mm. Therefore, this was defined as the minimal resolution for the method. The ability of the varnish to penetrate into the paper fibers for sealing the entire substrate structure was also examined. During the assays, it was concluded that stamping on only one side was sufficient to create an efficient hydrophobic barrier on both sides of the paper, as exposed in Fig. 3C. It may be attributed to the varnish's relatively low viscosity, which favors its quick penetration through the substrate. On the other hand, this relatively low viscosity was responsible for the lateral spread of the varnish observed during the stamping step, which caused an increase in the width of the hydrophobic barriers and a decrease in the width of the hydrophilic zones, in comparison with the nominal dimensions. The average width of the hydrophobic barriers of the PADs used in this work was 1.7 ± 0.1 mm (for $n = 25$ measurements), while the thickness of the stamps used was 1 mm. Regarding the width of the hydrophilic zones, Fig. 3D displays that for devices where the nominal dimensions were defined as 4, 5, 6, and 7 mm, the measured widths were 3.1 (78% of nominal size), 4.0 (80% of nominal size), 5.3 (88% of nominal size), and 6.4 (91% of nominal size), respectively (for $n = 5$ measurements in each size). These data indicate that there is a systematic deviation in the dimensional fidelity of the proposed protocol, being more accentuated for the smaller dimensions. However, it does not preclude the use of this procedure.

Morphological investigation

SEM was used to confirm the feasibility of using the varnish to create hydrophobic barriers on paper substrates. Figure 4A displays SEM image of surface of a paper-based device fabricated by this method. It can be clearly seen that there are differences between the bare paper (hydrophilic region) and the region covered by the varnish (hydrophobic

Table 1 Comparison of the procedure based on all-purpose varnish and 3D-printed stamps reported here versus other contact stamping methods used to create hydrophobic barriers on paper substrates

Fabrication technique	Instrumentation required	Steps	Hydrophobic material	Suitable for electrochemical applications	Drawbacks	Ref. (year)
Patterning with rubber stamps	Custom-made rubber stamps	Stamping and drying at room temperature	Waterproof indelible ink	Not demonstrated	Not suitable for large scale; Compatibility with acid, bases, surfactants, and commonly used organic solvents not demonstrated	[16] (2020)
Hot embossing with metal stamp	Wax printer; Embossing machine; Custom metal stamps	Prepare lab-engineered paper sheets; Coat paper with wax; Hot embossing with metal stamp patterns	Wax	Not demonstrated	Time consuming; Requires dedicated instrumentation; Not compatible with surfactants and common organic solvents [7, 20]	[17] 2019
Stamping with rubber patterns and nail polish	Custom magnet rubber stamper made by laser cutting	Dilute nail polish in ethyl acetate; Stamping and drying at room temperature	Nail polish	Not demonstrated	Not suitable for large scale; Not totally compatible with ethanol; Compatibility with acidic and other organic solvents not demonstrated	[18] (2018)
Stamping with Rubik's Cube and iron components	Rubik's Cube; Iron plates with laser-engraved patterns	Stamping and drying at room temperature	Rosin solution	Not demonstrated	Not suitable for large scale; Compatibility with acid, bases, surfactants, and commonly used organic solvents not demonstrated	[19] (2017)
Patterning with custom rubber stamps and PDMS	Elastomeric stamps; Oven	PDMS preparation; Stamping; Curing at oven	PDMS	Yes	Not suitable for large scale; Uses a toxic solvent (hexane)	[20] (2015)
Stamping with all-purpose varnish	3D-printed stamps	Stamping and drying at room temperature	Acrylic resin	Yes	Not suitable for large scale; Low resolution	This work

section), which confirms that the varnish successfully covers and seals the paper surface. Furthermore, Fig. 4B presents a cross-section image of PAD where it is evident that the varnish also permeates into the paper fibers to completely seal the desired regions of substrate, generating efficient hydrophobic barriers.

Chemical compatibility

The resistance of the hydrophobic barriers was investigated against various aqueous and organic media often used in analytical protocols. As shown in Fig. S3 (ESI), the varnish barriers presented optimal resistance in the pH range from 2

to 14. Moreover, the devices also showed good compatibility with aqueous solutions of neutral, cationic, and anionic surfactants (Triton X-100, CTAB, and SDS, respectively). This is especially interesting to the field of electroanalysis, where surfactants are often employed [30].

The varnish barriers were also tested against acetone, acetonitrile, ethanol, and methanol. None of these solvents affected the hydrophobic structures of the devices. This is an interesting finding since these solvents are commonly used in a variety of analytical procedures, such as non-aqueous electrophoresis and chromatography. The novel contact stamping method presented here showed better chemical resistance compared to other stamping methods,

Fig. 3 Spot tests (A) and fluidic channel devices (B) used to investigate the protocol resolution; front and back views of a lateral flow device fabricated and its respective stamp (C); comparison between nominal and real widths of hydrophilic zones in devices fabricated in several sizes (D). Each point on this plot was obtained from measurements of $n=5$ devices

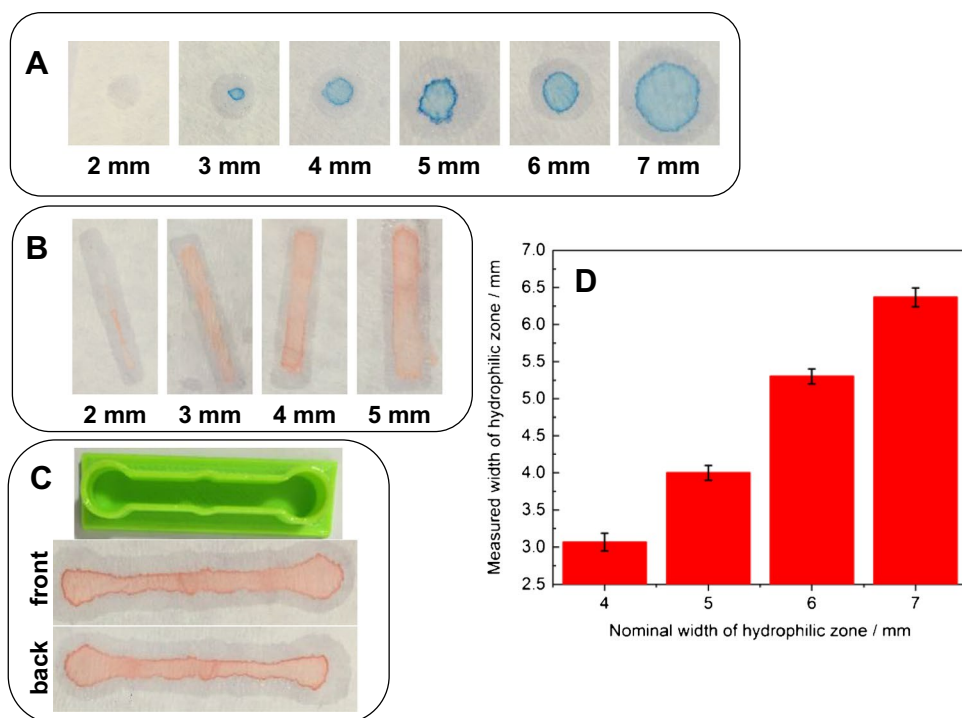
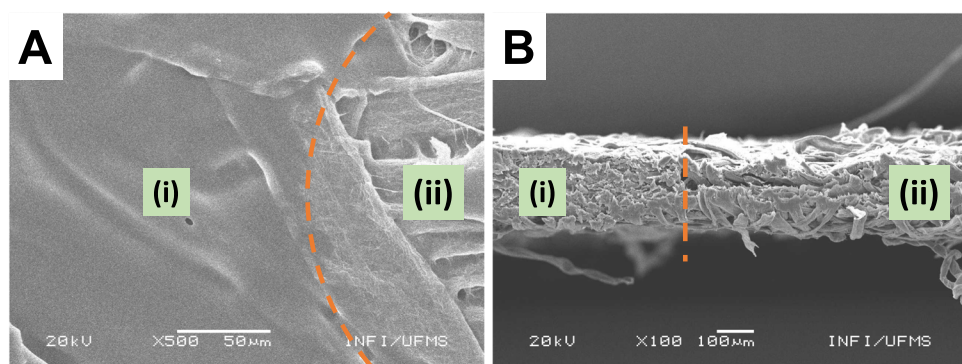


Fig. 4 SEM images of paper-based devices fabricated according to the described protocol: surface (A) and cross-section (B) image of a paper device; (i) refers to the hydrophobic barrier region and (ii) refers to the hydrophilic zone region of the device. The dashed lines indicate the separation between hydrophobic and hydrophilic zones



as summarized in Table 1. It opens up the possibilities for using this fabrication protocol for production of devices that can be applied in a wide range of aqueous and non-aqueous analytical procedures that are not covered by other stamping methods nor by well-established methods such as wax printing.

Flow characterization

The type the flow occurring into the channels fabricated by this stamping method was studied, since the theoretical understanding of the flow properties is an important matter regarding applications in microfluidics, where a laminar flow is expected. The dimensionless Reynolds' number (R_e) is an important criterion that describes whether such developed flow conditions lead to laminar or turbulent flow. It also

depends on the flow geometry and flow pattern. Reynolds' number is defined as:

$$R_e = \frac{\rho L U}{\mu}$$

in which ρ is the density of the fluid (kg m^{-3}), L is the width of the channel (m), U is the velocity of the flow (m s^{-1}), and μ is the dynamic viscosity of the fluid ($\text{kg m}^{-1} \text{s}^{-1}$). Values of R_e below 1000 suggest a laminar flow, whereas values of R_e above 1000 indicate a turbulent flow [31]. Using fluidic channels with the minimal resolution of the method (3 mm), aqueous media and the values of 1000 kg m^{-3} for ρ , $1 \times 10^{-3} \text{ kg m}^{-1} \text{ s}^{-1}$ for μ , and $3.14 \times 10^{-3} \text{ m s}^{-1}$ as the measured flow speed, the calculations yielded a R_e of ca. 6.3. This value indicates that the microfluidic paper devices demonstrated here produce a laminar flow, as expected.

Exploration of more complex shapes, flexibility, and electrochemical detection

Aiming to demonstrate the versatility of this fabrication approach, PADS with more complex geometries were fabricated as a proof of principle. As demonstrated in Fig. 5A, the stamping method based on 3D printing reported here is suitable for the fabrication of functional PADS in several shapes. Different geometries can be achieved according to the user demand at an affordable price. The cost of each 3D-printed stamp was appraised as *ca.* \$ 0.15. These devices might be employed in several applications, such as multiplexed analysis [32, 33]. Moreover, the PADs developed here presented excellent flexibility. As exhibited in Fig. S4 (ESI), the devices can be bent at an angle of 180° without damaging the hydrophobic structures. This feature makes this technology suitable for use on production of wearable sensors and demonstrates another great potentiality [34, 35].

Electrochemical techniques are quite interesting for detection in paper-based devices due to the selectivity and high sensitivity that can be achieved. The fabrication of paper-based electrochemical devices involves the incorporation of electrochemical sensors and delimitation of hydrophobic barriers. In this context, wax printing is the most used method for patterning paper substrates [36]. However, wax has as limitation its incompatibility with surfactants and organic solvents often used in electrochemical procedures, such as ethanol, methanol, and acetonitrile [37, 38]. So, protocols that allow the patterning of paper substrates with barriers that are compatible with organic media and surfactants are welcome and can enable electrochemical applications that cannot be performed with wax printing

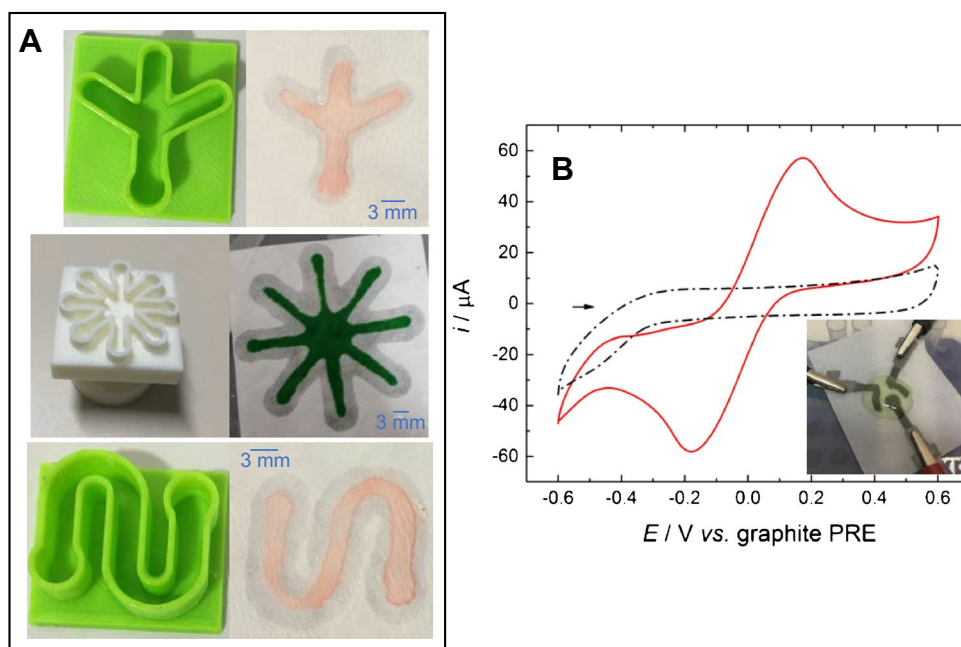
or other stamping methods. Voltammetric measurements using paper-based electrochemical devices fabricated according to the protocol described here were carried out in the presence of the benchmark redox system $\text{Fe}(\text{CN})_6^{4-}/\text{Fe}(\text{CN})_6^{3-}$. As can be seen in Fig. 5B, the voltammetric profile observed was well defined and as expected for such electrochemical system. Two peaks were obtained, one anodic at $E_p = +0.168$ V and one cathodic at $E_p = -0.175$ V [29, 39–41]. In addition, none unknown voltammetric signal was observed in the measurement of blank (0.5 mol L^{-1} KCl solution), indicating that the varnish hydrophobic barrier does not cause any interference in the voltammetric scans. These findings attest to the applicability of this contact stamping method for production of paper-based devices aiming electrochemical applications in aqueous and non-aqueous media, besides presenting evident advantages over other fabrication protocols such as simplicity and low cost.

Repeatability, reproducibility, and shelf life

Repeatability of the fabrication protocol was evaluated by assessing the diameter of the detection zones and the amount of all-purpose varnish transferred to each device in a series of $n = 10$ PADs fabricated using the same 3D-printed stamp. The observed relative standard deviation (*RSD*) was 6.2% regarding the diameter of the hydrophilic zones and 7.6% regarding the mass of varnish. These values are quite acceptable and indicate satisfactory fidelity among the devices.

Reproducibility was assessed in the same way. The diameter of hydrophilic zones and amount of varnish transferred to paper devices fabricated with $n = 6$ different 3D-printed stamps were compared. The *RSD* values achieved in these

Fig. 5 **A** Some functional paper-fluidic devices fabricated by the method proposed here and their respective 3D-printed stamps; **B** cyclic voltammograms recorded in the absence (dashed line) and presence (solid line) of 1 mmol L^{-1} each of potassium hexacyanoferrate(II) and potassium hexacyanoferrate(III). Electrolyte was 0.5 mol L^{-1} KCl solution. Measurements were recorded with the PED fabricated using the proposed stamping approach. Scan rate was 50 mV s^{-1}



assessments were 5.5 and 6.7%, respectively. These data indicate an acceptable reproducibility for the fabrication protocol. The normalized results of these assays are depicted in Fig. S5 (ESI). The PADs fabricated according to this method also showed long shelf life. If stored in a dry and contamination-free place, they remain usable for long periods (more than a year according to our studies).

Quantitative assays

As proof of concept to demonstrate feasibility in routine applications, spot tests fabricated according to the protocol developed here were used to quantify iron ions in pharmaceuticals by external standard method. The calibration plot obtained is presented in Fig. 6, where it can be seen that the colorimetric signal showed good dependence with concentration in the range from 2 until 25 mg L⁻¹. The corresponding linear equation was (Adjusted color intensity/AU) = $-(0.093 \pm 0.005) + (3.36 \pm 0.14) \times [\text{Fe}^{2+}]/\text{mg L}^{-1}$ and the correlation coefficient was 0.999. The values found for the limit of detection (LOD) and limit of quantification (LOQ) were 0.61 and 2.0 mg L⁻¹, respectively. The LOD was assessed experimentally (based on a signal-to-noise ratio of 3) while the LOQ was determined by the relationship $LOQ = 3.3 \times LOD$ [42, 43]. The LOD achieved in this current work is lower than the values reported by Waller in 2019 [22] and De Matteis in 2020 [44], who also utilized paper-based colorimetric platforms for iron sensing.

The analysis of three pharmaceuticals was carried out to certify the content of active ingredient using paper-based colorimetric sensors and also spectrophotometry, employed

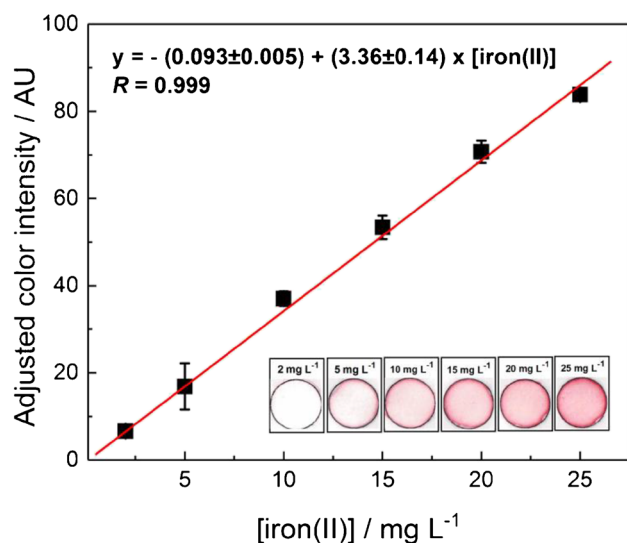


Fig. 6 Calibration plot obtained for image-based colorimetric measurements of Fe²⁺ ion using paper-based devices. Each dot is the average color intensity of $n=3$ individual measurements. The colorimetric responses were adjusted by subtracting the blank signal

as a reference method. The results obtained by the two methods were quite similar (the relative error was $<5\%$ for all measurements). Furthermore, the values found were in good agreement with the nominal content informed in the leaflets of the products (recoveries ranged between 104 and 108%). According to the legislation of Brazilian National Agency of Sanitary Surveillance (ANVISA), pharmaceutical formulations must have a real content of active ingredient ranging between 90 and 110% of the value informed in the leaflet [30]. Based on this legislation, the results obtained during the assays are within expectations and indicate satisfactory accuracy, as well as good precision ($RSDs$ were $<4\%$ for all measurements). These results are summarized in Table S1 (ESI) and prove the potential of this simple and inexpensive technology for use in routine analytical procedures, especially in resource-limited places.

Conclusions

This work has reported, for the first time, the use of all-purpose varnish and 3D-printed stamps for patterning hydrophobic barriers aiming the production of paper-based analytical platforms. This acrylic varnish is commonly used in craftwork and is sold worldwide at an affordable price (ca. \$ 27 per liter). The contact stamping method shown here allows applications in aqueous and non-aqueous media that are not possible with other methods. In addition, this stamping method also enabled the fabrication of paper electrochemical devices, showing great versatility. However, some limitations are the fact that it is not suitable for mass production and the resolution obtained is lower than those claimed by other methods. Our research group has been working on some strategies to improve the manufacturing process and implement large-scale production. About poor resolution compared to other methods, it is not a big issue, as devices manufactured by this method suit most applications.

The usefulness of this approach has been successfully demonstrated through quantitative determination of iron ions in pharmaceutical formulations. Thus, based on that described here, we believe this novel contact stamping method exhibits great potential for application in colorimetric and electrochemical measurements and is a very interesting option for fabrication of inexpensive point-of-care devices. Moreover, it explores another great potentiality for using 3D printing technologies in analytical sciences.

Supplementary Information The online version contains supplementary material available at <https://doi.org/10.1007/s00604-021-05102-7>.

Acknowledgements The authors are also grateful to Multiuser Laboratory for Analysis of Materials (MULTILAM) of Physics Institute at Federal University of Mato Grosso do Sul (UFMS) for providing the equipment and technical support for SEM measurements.

Funding Authors thank the financial support given by Conselho Nacional de Desenvolvimento Científico e Tecnológico (CNPq) and Coordenação de Aperfeiçoamento de Pessoal de Nível Superior—Brasil (CAPES)—Finance code 001.

Declarations

Conflict of interest The authors declare no competing interests.

References

- Cate DM, Noblitt SD, Volckens J, Henry CS (2019) Multiplexed paper analytical device for quantification of metals using distance-based detection. *Lab Chip* 15:2808–2818. <https://doi.org/10.1039/C5LC00364D>
- Chiang CK, Kurniawan A, Kao CY, Wang MJ (2019) Single step and mask-free 3D wax printing of microfluidic paper-based analytical devices for glucose and nitrite assays. *Talanta* 194:837–845. <https://doi.org/10.1016/j.talanta.2018.10.104>
- Chen W, Fang X, Li H, Cao H, Kong J (2016) A simple paper-based colorimetric device for rapid mercury(II) assay. *Sci Rep* 6:31948. <https://doi.org/10.1038/srep31948>
- Petroni JM, Lucca BG, da Silva Júnior LC, Alves DCB, Ferreira VS (2017) Paper-based electrochemical devices coupled to external graphene-Cu nanoparticles modified solid electrode through meniscus configuration and their use in biological analysis. *Electroanalysis* 29:2628–2637. <https://doi.org/10.1002/elan.20170398>
- da Silva GO, de Araujo WR, Paixao T (2018) Portable and low-cost colorimetric office paper-based device for phenacetin detection in seized cocaine samples. *Talanta* 176:674–678. <https://doi.org/10.1016/j.talanta.2017.08.082>
- Almeida M, Jayawardane BM, Kolev SD, McKelvie ID (2018) Developments of microfluidic paper-based analytical devices (muPADs) for water analysis: a review. *Talanta* 177:176–190. <https://doi.org/10.1016/j.talanta.2017.08.072>
- Sousa LR, Duarte LC, Coltro WKT (2020) Instrument-free fabrication of microfluidic paper-based analytical devices through 3D pen drawing. *Sensors Actuators B Chem* 312:128018. <https://doi.org/10.1016/j.snb.2020.128018>
- Martinez AW, Phillips ST, Wiley BJ, Gupta M, Whitesides GM (2008) FLASH: a rapid method for prototyping paper-based microfluidic devices. *Lab Chip* 8:2146–2150. <https://doi.org/10.1039/B811135A>
- Dossi N, Toniolo R, Terzi F, Sdrigotti N, Tubaro F, Bontempelli G (2018) A cotton thread fluidic device with a wall-jet pencil-drawn paper based dual electrode detector. *Anal Chim Acta* 1040:74–80. <https://doi.org/10.1016/j.aca.2018.06.061>
- de Tarso GP, Cardoso TMG, Garcia CD, Carrilho E, Coltro WKT (2014) A handheld stamping process to fabricate microfluidic paper-based analytical devices with chemically modified surface for clinical assays. *RSC Adv* 4:37637–37644. <https://doi.org/10.1039/C4RA07112C>
- Liu W, Guo Y, Li H, Zhao M, Lai Z, Li B (2015) A paper-based chemiluminescence device for the determination of ofloxacin. *Spectrochim Acta A Mol Biomol Spectrosc* 137:1298–1303. <https://doi.org/10.1016/j.saa.2014.09.059>
- Sameenoi Y, Nongkai PN, Nouanthavong S, Henry CS, Nacapracha D (2014) One-step polymer screen-printing for microfluidic paper-based analytical device (muPAD) fabrication. *Analyst* 139:6580–6588. <https://doi.org/10.1039/C4AN01624F>
- Fenton EM, Mascarenas MR, López GP, Sibbett SS (2009) Multiplex lateral-flow test strips fabricated by two-dimensional shaping. *ACS Appl Mater Interfaces* 1:124–129. <https://doi.org/10.1021/am800043z>
- Juang Y-J, Chen P-S, Wang Y (2019) Rapid fabrication of microfluidic paper-based analytical devices by microembossing. *Sensors Actuators B Chem* 283:87–92. <https://doi.org/10.1016/j.snb.2018.12.004>
- Ogihara H, Xie J, Okagaki J, Saji T (2012) Simple method for preparing superhydrophobic paper: spray-deposited hydrophobic silica nanoparticle coatings exhibit high water-repellency and transparency. *Langmuir* 28:4605–4608. <https://doi.org/10.1021/la204492q>
- Mathaweansurn A, Thongrod S, Khongkaew P, Phechkrajang CM, Wilairat P, Choengchan N (2020) Simple and fast fabrication of microfluidic paper-based analytical device by contact stamping for multiple-point standard addition assay: application to direct analysis of urinary creatinine. *Talanta* 210:120675. <https://doi.org/10.1016/j.talanta.2019.120675>
- Postulka N, Striegel A, Krauß M, Mager D, Spiehl D, Meckel T, Worgull M, Biesalski M (2019) Combining wax printing with hot embossing for the design of geometrically well-defined microfluidic papers. *ACS Appl Mater Interfaces* 11:4578–4587. <https://doi.org/10.1021/acsami.8b18133>
- Satarpai T, Siripinyanon A (2018) Alternative patterning methods for paper-based analytical devices using nail polish as a hydrophobic reagent. *Anal Sci* 34:605–612
- Fu H, Yang J, Guo L, Nie J, Yin Q, Zhang L, Zhang Y (2017) Using the Rubik's Cube to directly produce paper analytical devices for quantitative point-of-care aptamer-based assays. *Biosens Bioelectron* 96:194–200. <https://doi.org/10.1016/j.bios.2017.05.012>
- Dornelas KL, Dossi N, Piccin E (2015) A simple method for patterning poly(dimethylsiloxane) barriers in paper using contact-printing with low-cost rubber stamps. *Anal Chim Acta* 858:82–90. <https://doi.org/10.1016/j.aca.2014.11.025>
- Kang JH, Kim C (2018) Colorimetric detection of iron and fluorescence detection of zinc and cadmium by a chemosensor containing a bio-friendly octopamine. *Photochem Photobiol Sci* 17:442–452. <https://doi.org/10.1039/c7pp00468k>
- Waller AW, Toc M, Rigsby DJ, Gaytán-Martínez M, Andrade JW (2019) Development of a paper-based sensor compatible with a mobile phone for the detection of common iron formulas used in fortified foods within resource-limited settings. *Nutrients* 11:1673. <https://doi.org/10.3390/nu11071673>
- Lee S, Uliana A, Taylor MK, Chakarawet K, Bandaru SRS, Gul S, Xu J, Ackerman CM, Chatterjee R, Furukawa H, Reimer JA, Yano J, Gadgil A, Long GJ, Grandjean F, Long JR, Chang CJ (2019) Iron detection and remediation with a functionalized porous polymer applied to environmental water samples. *Chem Sci* 10:6651–6660. <https://doi.org/10.1039/C9SC01441A>
- Ambrosi A, Pumera M (2016) 3D-printing technologies for electrochemical applications. *Chem Soc Rev* 45:2740–2755. <https://doi.org/10.1039/C5CS00714C>
- Nesterenko PN (2020) 3D printing in analytical chemistry: current state and future. *Pure Appl Chem* 92:1341–1355. <https://doi.org/10.1515/pac-2020-0206>
- Li B, Fu L, Zhang W, Feng W, Chen L (2014) Portable paper-based device for quantitative colorimetric assays relying on light reflectance principle. *Electrophoresis* 35:1152–1159. <https://doi.org/10.1002/elps.201300583>
- Aguilar LG, Petroni JM, Ferreira VS, Lucca BG (2020) Easy and rapid pen-on-paper protocol for fabrication of paper analytical devices using inexpensive acrylate-based plastic welding repair kit. *Talanta* 219:121246. <https://doi.org/10.1016/j.talanta.2020.121246>
- de Mello Gabriel GV, Pitombo LM, Rosa LMT, Navarrete AA, Botero WG, do Carmo JB, de Oliveira LC (2021) The

- environmental importance of iron speciation in soils: evaluation of classic methodologies. *Environ Monit Assess* 193:63. <https://doi.org/10.1007/s10661-021-08874-w>
29. de França CCL, Meneses D, Silva ACA, Dantas NO, de Abreu FC, Petroni JM, Lucca BG (2021) Development of novel paper-based electrochemical device modified with CdSe/CdS magic-sized quantum dots and application for the sensing of dopamine. *Electrochim Acta* 367:137486. <https://doi.org/10.1016/j.electacta.2020.137486>
 30. de Jesus VO, Ferreira VS, Lucca BG (2020) Electrochemical study and simultaneous voltammetric determination of contraceptives ethinylestradiol and cyproterone acetate using silver nanoparticles solid amalgam electrode and cationic surfactant. *Talanta* 210:120610. <https://doi.org/10.1016/j.talanta.2019.120610>
 31. Oyola-Reynoso S, Frankiewicz C, Chang B, Chen J, Bloch JF, Thuo MM (2017) Paper-based microfluidic devices by asymmetric calendaring. *Biomicrofluidics* 11:014104. <https://doi.org/10.1063/1.4974013>
 32. Feng L-X, Tang C, Han X-X, Zhang H-C, Guo F-N, Yang T, Wang J-H (2021) Simultaneous and sensitive detection of multiple small biological molecules by microfluidic paper-based analytical device integrated with zinc oxide nanorods. *Talanta* 232:122499. <https://doi.org/10.1016/j.talanta.2021.122499>
 33. Han DK, Oh J, Lee J, Cho YG, Park JS, Choi JS, Kim DS, Kwon J (2021) Paper-based multiplex analytical device for simultaneous detection of *Clostridioides difficile* toxins and glutamate dehydrogenase. *Biosens Bioelectron* 176:112894. <https://doi.org/10.1016/j.bios.2020.112894>
 34. de Castro LF, de Freitas SV, Duarte LC, de Souza JAC, Paixão TRLC, Coltro WKT (2019) Salivary diagnostics on paper microfluidic devices and their use as wearable sensors for glucose monitoring. *Anal Bioanal Chem* 411:4919–4928. <https://doi.org/10.1007/s00216-019-01788-0>
 35. Li M, Wang L, Liu R, Li J, Zhang Q, Shi G, Li Y, Hou C, Wang H (2021) A highly integrated sensing paper for wearable electrochemical sweat analysis. *Biosens Bioelectron* 174:112828. <https://doi.org/10.1016/j.bios.2020.112828>
 36. Noviana E, Henry CS (2020) Simultaneous electrochemical detection in paper-based analytical devices. *Curr Opin Electrochem* 23:1–6. <https://doi.org/10.1016/j.coelec.2020.02.013>
 37. Stanić Z, Dimić T, Simić Z, Jakšić L, Girousi S (2011) Electrochemical characterization and analytical application of arsenopyrite mineral in non-aqueous solutions by voltammetry and potentiometry. *Polyhedron* 30:702–707. <https://doi.org/10.1016/j.poly.2010.12.009>
 38. Trindade MAG, Bilibio U, Zanoni MVB (2014) Enhancement of voltammetric determination of quinizarine based on the adsorption at surfactant-adsorbed-layer in disposable electrodes. *Fuel* 136:201–207. <https://doi.org/10.1016/j.fuel.2014.07.044>
 39. Petroni JM, Neves MM, de Moraes NC, da Silva RAB, Ferreira VS, Lucca BG (2021) Development of highly sensitive electrochemical sensor using new graphite/acrylonitrile butadiene styrene conductive composite and 3D printing-based alternative fabrication protocol. *Anal Chim Acta* 1167:338566. <https://doi.org/10.1016/j.aca.2021.338566>
 40. de Moraes NC, da Silva ENT, Petroni JM, Ferreira VS, Lucca BG (2020) Design of novel, simple, and inexpensive 3D printing-based miniaturized electrochemical platform containing embedded disposable detector for analytical applications. *Electrophoresis* 41:278–286. <https://doi.org/10.1002/elps.201900270>
 41. Petroni JM, Lucca BG, Ferreira VS (2017) Simple and inexpensive electrochemical platform based on novel homemade carbon ink and its analytical application for determination of nitrite. *Electroanalysis* 29:1762–1771. <https://doi.org/10.1002/elan.201701117>
 42. Mocak J, Bond AM, Mitchell S, Scollary G (1997) A statistical overview of standard (IUPAC and ACS) and new procedures for determining the limits of detection and quantification: application to voltammetric and stripping techniques (Technical Report). *Pure Appl Chem* 69:297–328. <https://doi.org/10.1351/pac199769020297>
 43. da Silva ENT, Ferreira VS, Lucca BG (2019) Rapid and inexpensive method for the simple fabrication of PDMS-based electrochemical sensors for detection in microfluidic devices. *Electrophoresis* 40:1322–1330. <https://doi.org/10.1002/elps.201800478>
 44. De Matteis V, Cascione M, Fella G, Mazzotta L, Rinaldi R (2020) Colorimetric paper-based device for hazardous compounds detection in air and water: a proof of concept. *Sensors* 20:5502. <https://doi.org/10.3390/s20195502>

Publisher's note Springer Nature remains neutral with regard to jurisdictional claims in published maps and institutional affiliations.